

Short Note

Image segmentation with bounds

Jesse Lomask and Biondo Biondi¹

INTRODUCTION

Image segmentation (Shi and Malik, 2000; Hale and Emanuel, 2003, 2002) for tracking salt boundaries (Lomask and Biondi, 2003; Lomask et al., 2004) is extremely memory intensive. Memory saving measures must be implemented in order to consider applying this technique to 3D seismic cubes. If coarse bounds can be picked, either manually or using another automatic algorithm, this image segmentation algorithm can then be used to partition between the bounds. Unfortunately, the quality of the segmentation result is strongly affected by the shape of the image. For example, elongated images are more likely to be partitioned along their shortest dimension.

In this note, we present one such memory saving technique and demonstrate its ability to pick a salt boundary on a 2D seismic section. By imposing bounds, we significantly reduce the size of the problem and, as a result, increase efficiency and robustness. Also, errors created by segmenting thin images can be rectified with novel boundary conditions described here.

METHODOLOGY

Normalized cuts image segmentation partitions images into two groups. To do this, it first creates weights relating each sample to every other sample along paths within local neighborhoods. It then finds the cut that partitions the image into two groups, A and B , by minimizing the normalized cut:

$$N_{\text{cut}} = \frac{\text{cut}}{\text{total}_A} + \frac{\text{cut}}{\text{total}_B} \quad (1)$$

where cut is the sum of the weights cut by the partition. total_A is the sum of all weights in Group A , and total_B is the sum of all weights in Group B . Normalizing the cut by the sum of all the weights in each group prevents the partition from selecting overly-small groups of nodes.

¹email: lomask@sep.stanford.edu, biondo@sep.stanford.edu

The minimum of N_{cut} can be found by solving the generalized eigensystem:

$$(\mathbf{D} - \mathbf{W})\mathbf{y} = \lambda\mathbf{D}\mathbf{y}, \quad (2)$$

created from a weight matrix (\mathbf{W}) and a diagonal matrix (\mathbf{D}), with each value on the diagonal being the sum of each column of \mathbf{W} . The eigenvector (\mathbf{y}) with the second smallest eigenvalue (λ) is used to partition the image by taking all values greater than zero to be in one group, and its complement to be in the other. For a more detailed description, please see Shi and Malik (2000).

For application to seismic salt interfaces, we merely apply the algorithm to instantaneous amplitude. Several cost saving techniques are explored in Lomask et al. (2004).

By applying bounds we greatly reduce the size of the problem. These initial rough bounds can be found by first running the algorithm with small search neighborhoods and coarse sampling.

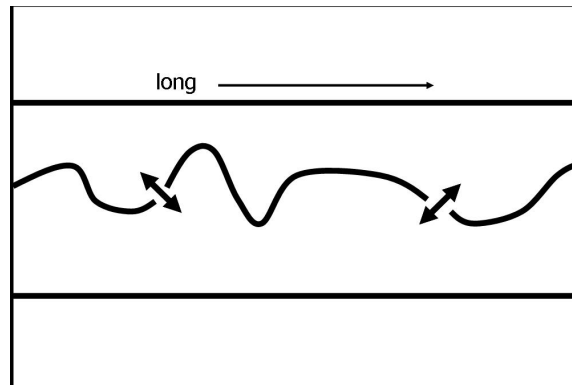


Figure 1: A cartoon of a masked salt boundary. It is long and thin with a discontinuous salt boundary snaking across it. [jesse3-pic2](#) [NR]

Unfortunately, the normalized cut segmentation method tends to partition elongated images along their shortest dimension. For instance, Figure 1 is a cartoon of an elongated image with a salt boundary snaking across it. If the segmentation algorithm were to function as hoped, the minimum cut would be found along the salt boundary. However, because the salt boundary is discontinuous, it is likely that the minimum of the normalized cut in equation (1) will be found by cutting the image vertically where the image is thin.

To correct this problem, we exploit the fact that the upper boundary will necessarily be in Group A and the lower boundary will be in Group B . In other words, we want to force the segmentation algorithm to put the coarsely picked bounds in different groups.

We can enforce this constraint during the creation of the weight matrix (\mathbf{W}). Recall that this matrix contains weights relating each sample to every other sample along paths within a neighborhood. For any given sample, if its search neighborhood happens to cross a coarse boundary, it becomes weighted to every other sample near the boundary. This can be imagined by wrapping the image on a globe so that both the upper and lower bounds collapse to points at the poles (see Figure 2). When estimating the weight matrix, every time a path crosses the north or south pole, it continues down the other side. In Cartesian space, this can be seen in the cartoon in Figure 3.

Figure 2: A cartoon illustrating global bounds. The image is stretched onto a sphere and the upper and lower boundaries of the mask collapse to points. [jesse3-pic6](#) [NR]

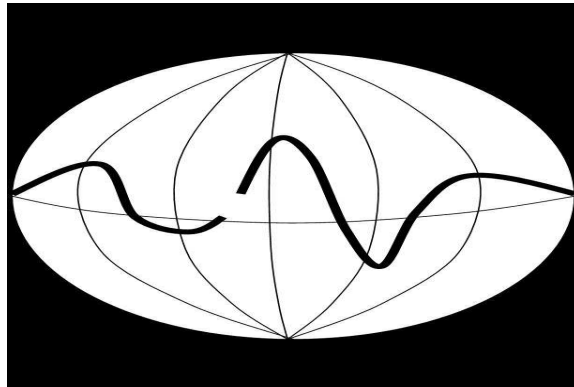
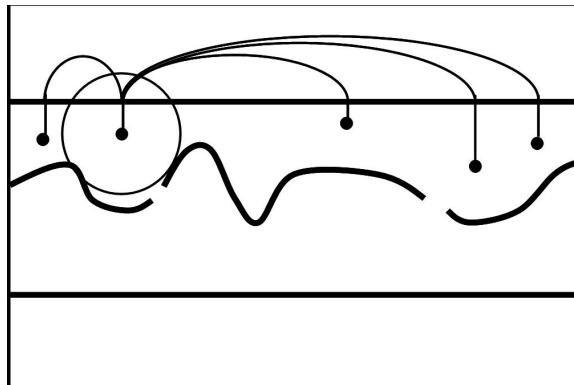


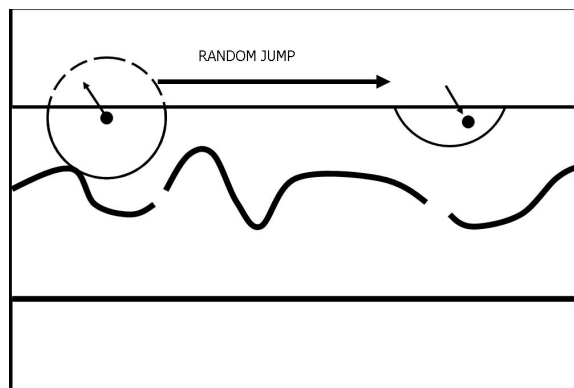
Figure 3: A cartoon illustrating idealized global bounds. When the search area for a node reaches outside the mask (as shown by the circle on the left), it becomes connected to all points along the boundary. [jesse3-pic5](#) [NR]



This “Global” bounds approach is completely impractical because it creates as many new weights as are saved by the size reduction of the problem.

A more practical approach that is still essentially the same concept is “Random” bounds. This is illustrated in Figure 4. Every time a path crosses a bound, it jumps a random distance along the boundary.

Figure 4: A cartoon illustrating the more practical random bounds. When the search area for a node reaches outside the mask (as shown by the circle on the left), it is connected to a single node a random distance along the boundary. [jesse3-pic4](#) [NR]



We have implemented and tested this random bounds method and found that it works well in our preliminary test cases.

FIELD TEST CASE

We tested this method on a 2D section taken from a Gulf of Mexico data set provided by WesternGeco.

Figure 5 shows a base of salt reflection. Although it is discontinuous, the human eye can see how it should be picked without too much uncertainty.

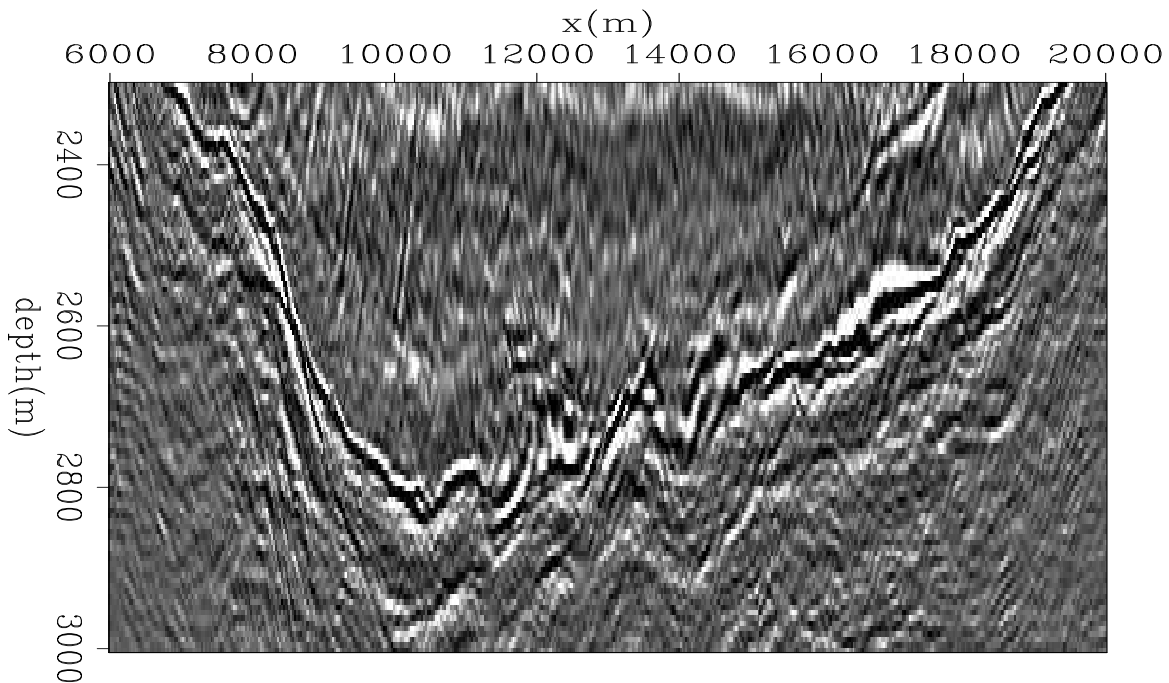


Figure 5: A 2D seismic section with a salt boundary from the Gulf of Mexico. `jesse3-gom.data` [ER]

We first ran the standard segmentation method on the entire image in Figure 5 with a short search distance and coarse sampling. We then shifted the result up and down 20 samples to get the mask shown in Figure 6.

Now our image is thinner and defined by that mask. We ran the standard segmentation method on the masked area. The resulting eigenvector (y) used to partition the image is shown in Figure 7. In principle, this eigenvector would be clipped to track the salt. Unfortunately, it is dominated by a low frequency trend and will create an erroneous vertical cut.

The eigenvector result of applying the random bounds approach is shown in Figure 8. It is clear that the salt interface can be gleaned from this image.

The resulting tracked salt boundary is displayed in Figure 9. It does an excellent job of tracking the salt boundary. The base salt tracking result is also overlain on the full 2D section in Figure 10.

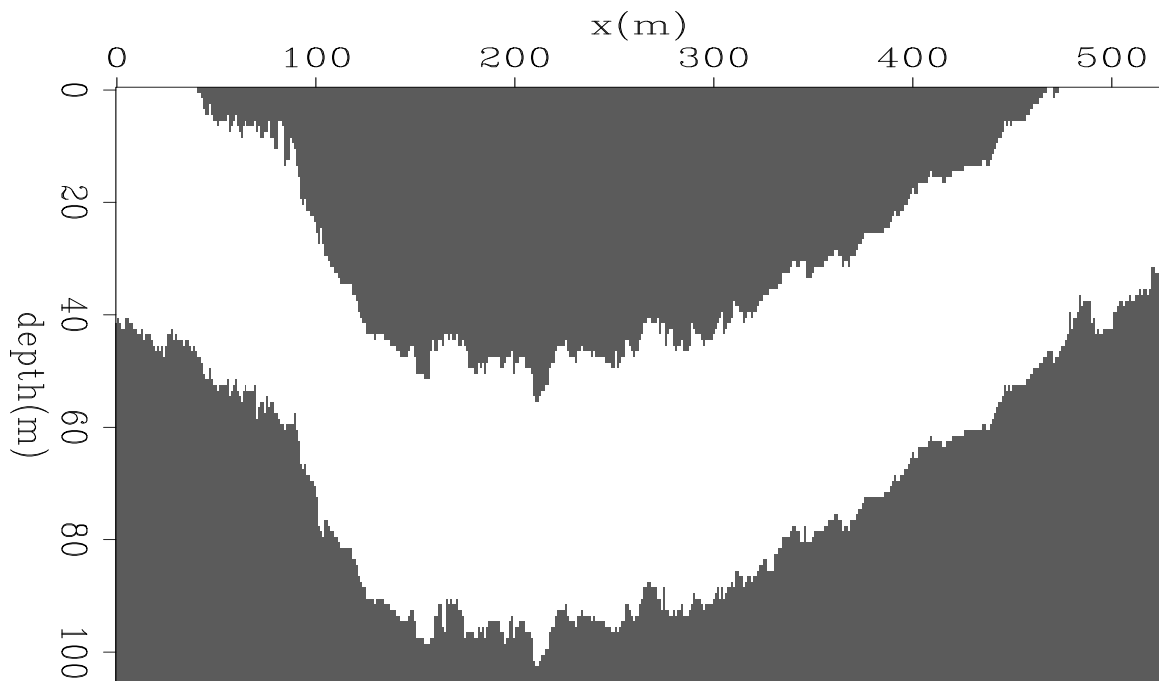


Figure 6: A binary mask defining the bounds of the salt boundary. This was generated by first running the image segmentation method on the entire image with short search distances and sparse sampling. In this case, the mask reduces the size of the problem by a factor of 2.

`jesse3-gom.mask_in` [ER]

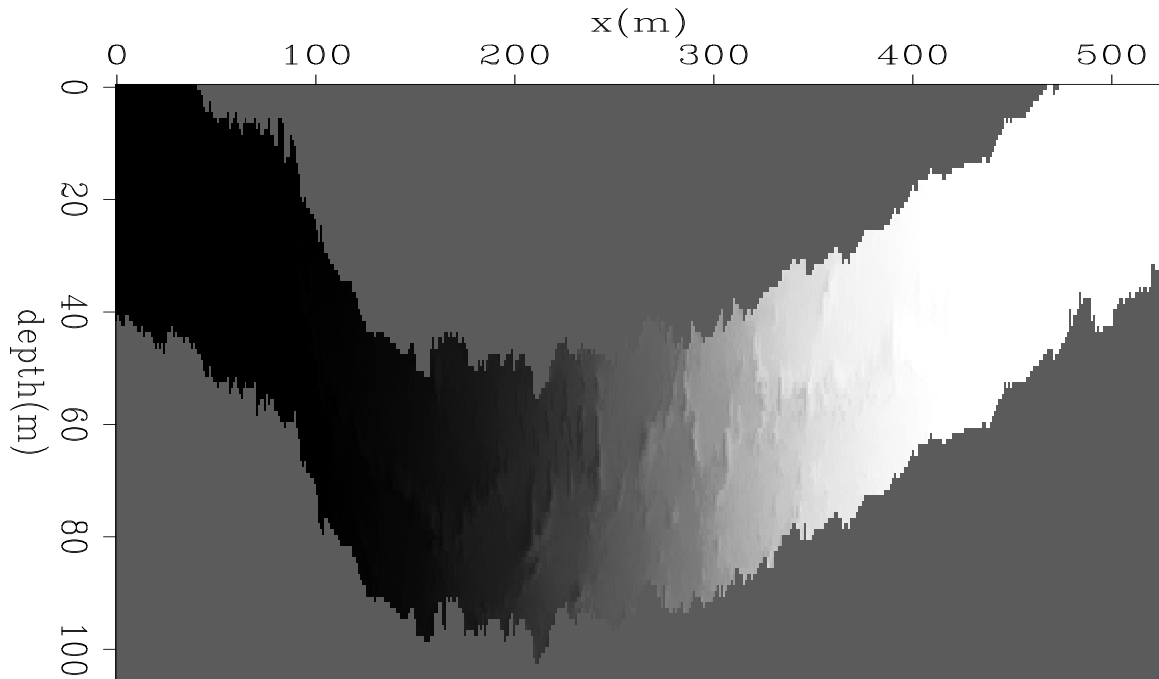


Figure 7: The eigenvector that is used to partition the image using our old segmentation algorithm after the mask in Figure 6 is applied. Hints of the salt boundary can be seen but is obscured by the overall low frequency trend from left to right. This will not produce a satisfactory segmentation result. `jesse3-gom.eig_nrand` [ER]

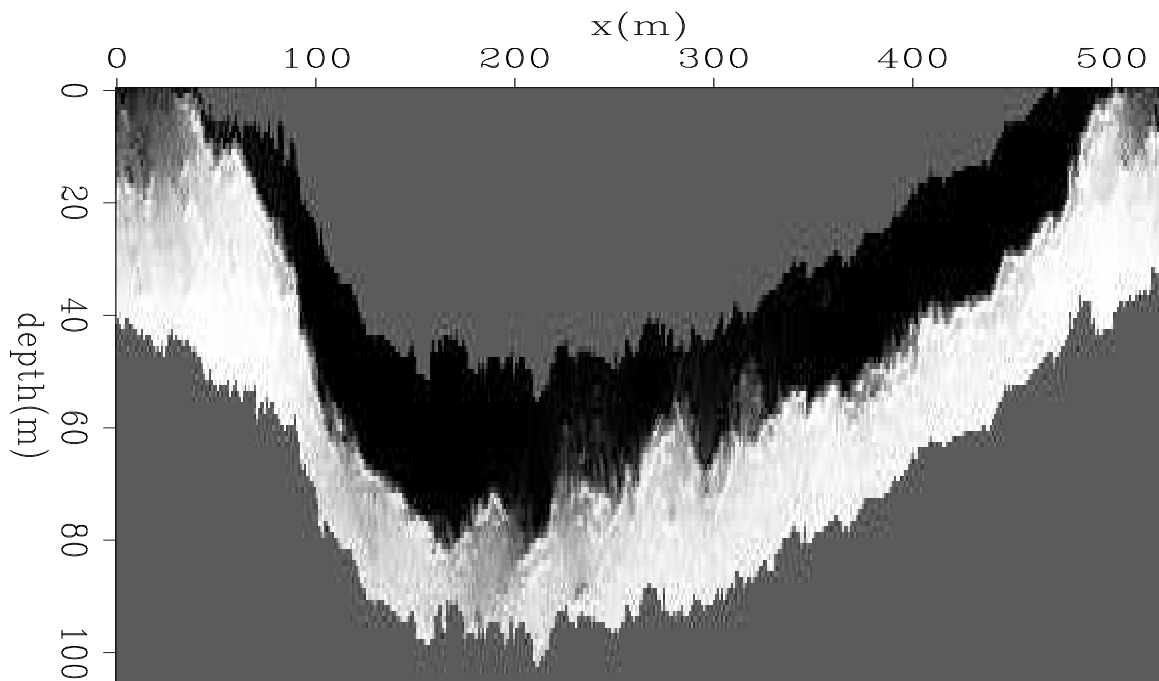


Figure 8: The eigenvector that is used to partition the image using our new approach with random bounds. The salt boundary is conspicuous in this image and can be extracted easily. `jesse3-gom.eig_rand` [ER]

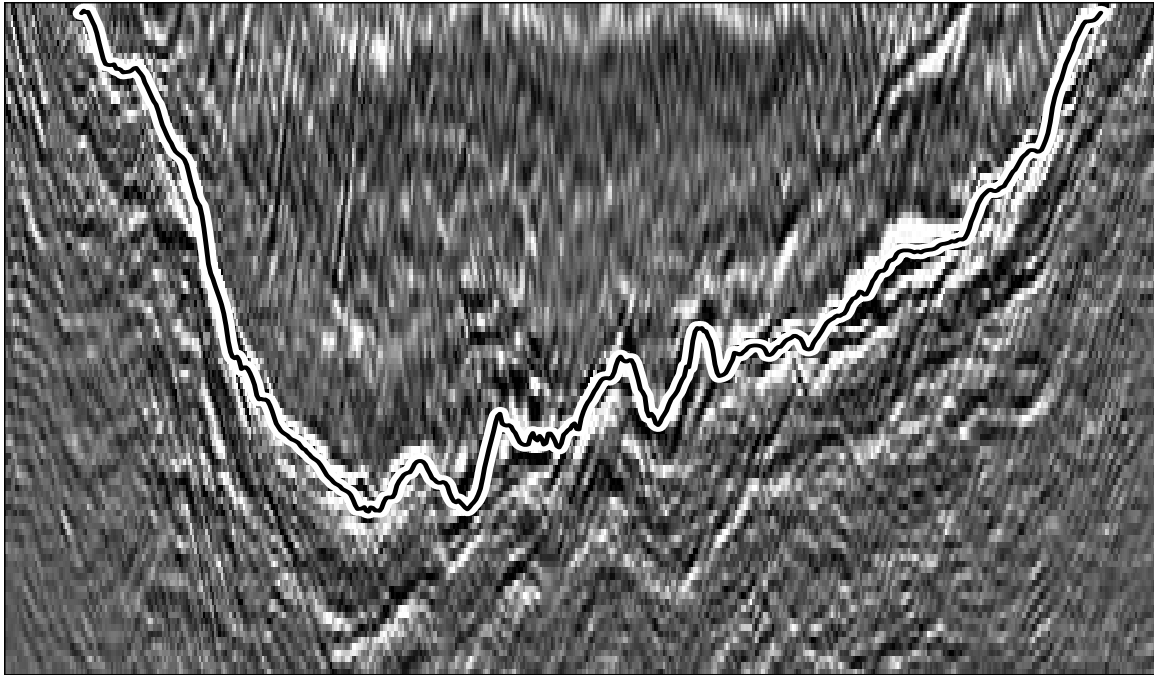


Figure 9: The boundary is garnered from the image in Figure 8 and overlain on the original base of salt data. It does a very good job of tracking the boundary. `jesse3-gom.horiz2` [ER]

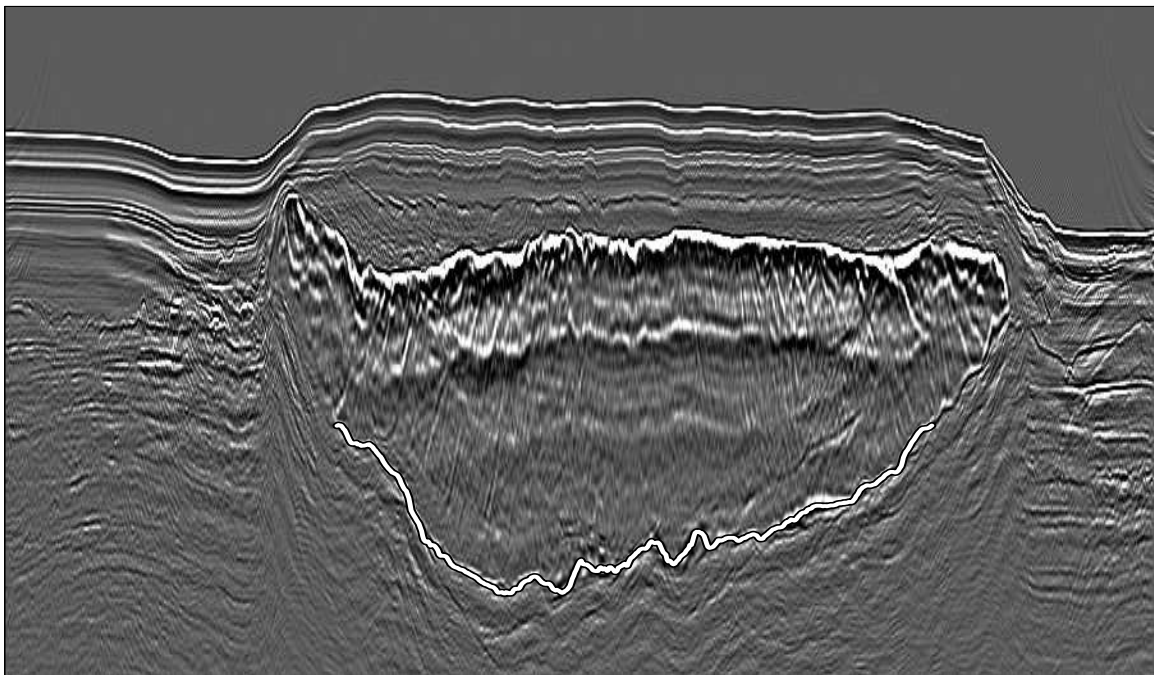


Figure 10: The boundary is overlain on a larger 2D section. `jesse3-gom_horiz2_full` [ER]

CONCLUSIONS

In this note, we presented a modification of image segmentation that allows narrow bounds to be introduced. We then demonstrated its effectiveness on a 2D field data set from the Gulf of Mexico. Now, armed with this new tool, tackling the 3D problem is one step closer.

ACKNOWLEDGMENT

We would like to thank WesternGeco for providing the field data used in this paper. We would also like to thank Dave Hale for his insightful suggestions.

REFERENCES

- Hale, D., and Emanuel, J. U., 2002, Atomic meshing of seismic images: Soc. of Expl. Geophys., Expanded Abstracts, 2126–2129.
- Hale, D., and Emanuel, J. U., 2003, Seismic interpretation using global image segmentation: Soc. of Expl. Geophys., Expanded Abstracts, 2410–2413.
- Lomask, J., and Biondi, B., 2003, Image segmentation for tracking salt boundaries: SEP-114, 193–200.
- Lomask, J., Biondi, B., and Shragge, J., 2004, Improved image segmentation for tracking salt boundaries: SEP-115, 357–366.
- Shi, J., and Malik, J., 2000, Normalized cuts and image segmentation: IEEE Trans on Pattern Analysis and Machine Intelligence, **22**, no. 8, 838–905.